CHEMBIOCHEM

DOI: 10.1002/cbic.200700351

Ligand-Induced Flocculation of Neurotoxic Fibrillar Aβ(1–42) by Noncovalent Crosslinking

Anasztázia Hetényi,[a] Lívia Fülöp,[b] Tamás A. Martinek,*[a] Edit Wéber,[a] Katalin Soós,[b] and Botond Penke*[b]

Aggregation of the amyloid-β (Aβ) peptides has a pivotal role in Alzheimer's disease (AD). Small molecules and short peptides/peptidomimetics can exert their full protective effects against Aβ within a short time-frame, but the exact mechanism of action is unclear. Time-dependent NMR spectroscopic binding and replacement experiments were carried out for peptide LPFFD and thioflavine T (ThT) on neurotoxic fibrillar Aβ(1–42), which revealed transient binding behavior for both compounds, and complex time-dependent features in the replacement experiments. The results of particle size measurements through the use of diffuse light-scattering and transmission electron microscopy support the conclusions that the studied ligands induced interfibrillar association on a short timescale, which explains the NMR spectroscopic binding and replacement results. ζ-Potential measurements revealed a slightly increased electrostatic stability of the Aβ fibrils upon ligand binding; this suggests that the interfibrillar assembly is driven by specific noncovalent cross-linking interactions. A specific surface and mobility decrease due to the ligand-induced flocculation of the Aβ fibrils can explain the neuroprotective effects.

Introduction

Two microscopic changes occur in the brain in Alzheimer's disease (AD): senile plaques develop between the neurons,[1] and neurofibrillary tangles develop within the neurons.[2] It is widely accepted that amyloid-β peptide (Aβ) aggregates play a central role in the progression of AD.[3–5] These specific Aβ assemblies contain amphipathic molecules that consist of 39–43 residues, which are formed during the enzymatic cleavage of the amyloid precursor protein. Aβ(1–40) is the most prevalent species, but Aβ(1–42) is more toxic.[6–9] A number of mechanisms have been proposed to explain the neurotoxicity of Aβ, but the cytotoxic mechanism is still not fully understood.[5,10–17] Aβ of uncharacterized aggregation state induces the loss of surface NMDA receptors over time[18] and impairs the functions of metabotropic glutamate receptors.[19] Experimental data strongly suggest that the aggregation state and conformation have a crucial effect on the mechanism of the neurotoxicity. Soluble Aβ oligomers inhibit long-term potentiation,[20] memory processes in rodent models[21] and activate a mitochondrial death apoptotic pathway.[22] Fibrillar Aβ induces neuritic dystrophy,[22] neuronal apoptosis,[23] activates microglia,[24] causes axonopathy via hyperphosphorylation, and dissociation of the microtubule-associated tau protein,[8,25] and rapidly enhance NMDA receptor function, while it ablates the AMPA-induced neuronal firing rate.[26] On the other hand, Aβ monomers are not associated with neuronal dysfunction, and Aβ plaques themselves do not cause memory impairment either, that is, until they occupy a substantial portion of the tissue volume in cerebral cortex and hippocampus.[27] The consensus might be that the harmful Aβ species are larger than monomers but smaller than the nonmobile superaggregates in plaques, and both oligomeric and fibrillar Aβ aggregates are targets for drug design in AD research.

Short peptides and small molecules can influence the structure and aggregation of Aβ, and these are effective neuroprotective agents.[1] Peptides that are partially homologous to the central hydrophobic region of Aβ (residues 17–21), but that contain amino acids that prevent the adoption of a β-sheet structure bind to Aβ and inhibit amyloid formation in vitro and disaggregate preformed Aβ fibrils.[28–34] The full β-sheet-breaking effect of these compounds on preaggregated Aβ fibrils takes place in a time-frame of several days; it can be detected by using thioflavine T (ThT) fluorometric staining, circular dichroism (CD) and transmission electron microscopy (TEM). On the other hand, cell viability (MTT tests) and electrophysiological measurements have clearly revealed that the protective effects of Aβ(17–21) analogues and other short neuroprotective peptides are exerted within 1 day (MTT tests) or even within 30 min (in vivo electrophysiology tests).[8,9,35,36] It is widely accepted that these molecules could be promising candidates to combat AD, but the exact nature of the interactions in a shorter time-frame remains elusive. The mechanism might comprise a partial β-sheet-breaking effect, or molecular surface covering that involves weak binding.[37–39]

[a] *Dr. A. Hetényi, Dr. T. A. Martinek, E. Wéber*
Institute of Pharmaceutical Chemistry, University of Szeged
Eötvös u. 6, 6720 Szeged (Hungary)
Fax: (+36) 62-545705
E-mail: martinek@pharm.u-szeged.hu

[b] *Dr. L. Fülöp, Dr. K. Soós, Prof. Dr. B. Penke*
Department of Medical Chemistry, University of Szeged
Dóm tér 8, 6720 Szeged (Hungary)

Supporting information for this article is available on the WWW under http://www.chembiochem.org or from the author.

Fibrillar Aβ is rich in β-sheet structure with hydrogen bonding between monomers that are parallel to the fibril axis; this leads to filaments of indefinite length.[40–43] Through this property, the amyloid fibrils can be studied via ThT fluorometric staining, because ThT can specifically interact with the crossed β-sheet structure[38,39,44–48] to give rise to a new excitation maximum and enhanced emission. Time-resolved experiments on Aβ(1–28) fibrils revealed that the fluorometric signal that were assigned to ThT binding decreased within a time-frame of 500 s under the conditions used.[44] The results were inconclusive as to whether the diminishing fluorescence signal was caused by decreased binding or structural changes.

The interactions of small molecules and peptides with Aβ can be monitored by surface plasmon resonance[49] and NMR spectroscopic techniques.[50–52] Transferred residual dipolar couplings (trRDC) and transferred NOE (trNOE) measurements indicated weak interactions between short neuroprotective peptides and Aβ(14–23).[52] trNOE experiments allowed the structures of the studied ligands in the bound state to be characterized, and the results demonstrate that the ligands bind to the long side of an Aβ fibril. NMR spectroscopic binding tests that are based on the signal quenching due to ligand association to large aggregates afforded estimates of the K_d values.

The goal of the present study was to improve our understanding of processes that are initiated by the binding of short neuroprotective peptides to fibrillar Aβ(1–42) within the time-frame of the above-mentioned biological tests. We set out to test the relevance of the results of NMR spectroscopic binding measurements with respect to the neuroprotective effects of Aβ(17–21) analogues and other peptides of Aβ origin that inhibit Aβ(1–42) toxicity. Our aim was to monitor the time-dependent changes in the binding of the most thoroughly studied β-sheet-breaker peptide, LPFFD to fibrillar Aβ(1–42). The time-dependent nature of the ThT binding was studied, and competition measurements with LPFFD were carried out. The flocculation (precipitation due to weak attracting forces between destabilized particles) and sedimentation of the fibrillar Aβ(1–42) particles in response to the binding of LPFFD and/or ThT were observed by NMR spectroscopy, TEM and diffuse light scattering methods, together with ζ-potential measurements.

Results

NMR spectroscopic binding tests on short neuroprotective peptides and fibrillar Aβ(1–42)

The efficiency and validity of the NMR spectroscopic binding experiment were tested on the short neuroprotective peptides LPFFD, LPYFD-NH_2, FRHDS-NH_2 and RIIGL-NH_2. The listed compounds exhibited neuroprotective effects in vitro in 3-(4,5-dimethylthiazole-2-yl)-2,5-diphenyl tetrazolium bromide (MTT), and in vivo in electrophysiology tests.[8,9,35,36] As a negative control, the practically inactive GGGGG-NH_2 was utilized. The NMR spectroscopic binding tests were carried out by using preformed mature fibrils of Aβ(1–42) as a target in a 1:5 Aβ(1–42)/ligand ratio. The signal intensity of the pure ligand in the ^{1}H NMR spectra was taken as 100%. The difference spectrum for LPFFD (the scaled ^{1}H spectrum of the pure ligand minus the ^{1}H spectrum of the ligand in the presence of fibrillar Aβ(1–42)) is displayed in Figure 1. The bound fraction for compounds that inhibit Aβ(1–42)-induced processes varied in the range of 9–26%, while no binding-related signal quenching was observed for the negative control of GGGGG-NH_2 (Table 1).

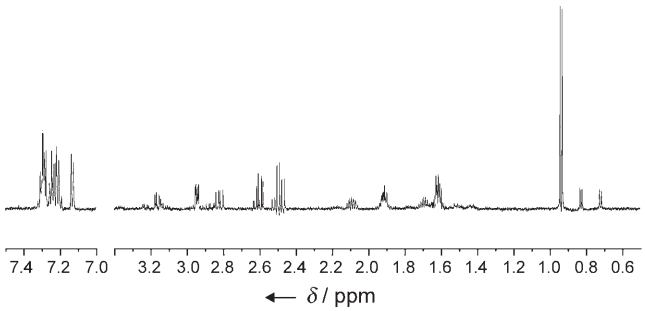

Figure 1. ^{1}H NMR difference spectrum of LPFFD upon binding to fibrillar Aβ(1–42).

Table 1. Comparison of the results on the neuroprotective effects of the studied peptides with their fractions bound to fibrillar Aβ(1–42) in NMR experiments.

Ligand	MTT cell viability test[a] [%]	Bound fraction[b] [%]
LPYFD-NH_2	92	19
FRHDS-NH_2	89	26
RIIGL-NH_2	86	9
LPFFD	84	17
GGGGG-NH_2	64	0

[a] Taken from refs. [8], [35] and [36]; data are referenced to a cell viability of 52% for fibrillar Aβ(1–42). [b] Values were obtained at the first measurement point.

From the ligand-binding ratios, weak millimolar dissociation constants (K_d) were computed by using the Hill–Langmuir equation with the assumption that one ligand is bound per Aβ(1–42) monomer. Because the exact number of binding sites per Aβ chain is not known a priori, complete dissociation curves were not recorded. For FRHDS-NH_2, the bound fraction exceeded the 1:1 limit. It should be noted that no significant line broadening was detected for the ligand resonances, which would otherwise be expected for the fast exchange of a weakly bound ligand.

The effect of the fibrillar Aβ(1–42) concentration was tested on LPFFD to validate the origin of the signal-quenching phenomenon. The bound fraction increased with elevation of the concentration of fibrillar Aβ(1–42) (Figure S1), but the response was nonlinear, which might be due to the low millimolar affinity and/or the complex structuring effect of the ligand (see later).

The fluorometric detection of ThT binding is a well-known means of indicating the β-sheet structure, and we therefore

made an attempt to characterize the ThT binding quantitatively with the NMR spectroscopy experiments that are described above. As expected, ThT readily bound to fibrillar Aβ(1–42); the ligand-binding ratio was 60% at the first measurement point, which indicates that 3 ThT molecules were bound to each Aβ(1–42) monomer.

Time-dependent binding and replacement experiments with LPFFD and ThT

The time-dependent binding features of the LPFFD–Aβ(1–42) sample were monitored for 24 h, and the ligand-binding ratio was found to converge from the initial 17% to a final value of 6% within 12 h (Figure 2A).

ThT has a relatively high affinity for Aβ fibrils (K_d ranging from high nM to low μM),[53,54] therefore the immediate replacement of LPFFD by ThT was expected if their binding sites overlap. Two samples were prepared: 1) LPFFD was mixed with fibrillar Aβ(1–42), and after 50 min ThT stock solution was added (sample B in Figure 2); and 2) ThT was mixed with fibrillar Aβ(1–42), and after 50 min LPFFD stock solution was added (sample C in Figure 2). Intriguingly, none of the samples exhibited full replacement immediately; however, lower bound fractions were observed for the peptide at the first measurement points, which indicates partial replacement. Moreover, the ThT-binding ratio increased significantly for both samples in the presence of LPFFD. For sample B (peptide added first), the rate of decrease was lower than that for the ThT–Aβ(1–42) sample, but a steeper domain was still present during the first 3 h. After 17 h, the bound fraction of LPFFD was zero, while the ThT binding ratio had dropped from the initial 74% to 47%, both values are significantly higher than the binding ratios that were observed for the ThT–Aβ(1–42) system. For sample C (ThT added first), the decreased rate pattern was very similar to that for the ThT–Aβ(1–42) mixture. Soon after 3 h, the LPFFD-binding ratio attained a negligibly low value, but the ThT-bound fraction dropped from the initial 66% to 35%, which are values that are slightly higher than those for the ThT–Aβ-(1–42) system. The trend of the decrease is best fitted with a linear relationship, and values are given in the caption of Figure 2. As a control experiment, saturation transfer difference (STD) spectra were recorded on the resuspended samples, which corroborated the existence of the binding between the fibrillar Aβ(1–42) and the ligands studied (Figure S2). On the other hand, a mixture of LPFFD and ThT in the absence of Aβ-(1–42) was monitored, and no signal quenching was observed.

Because precipitates were observed at the bottom of the test tubes, and floccules were attached to the tube wall in all

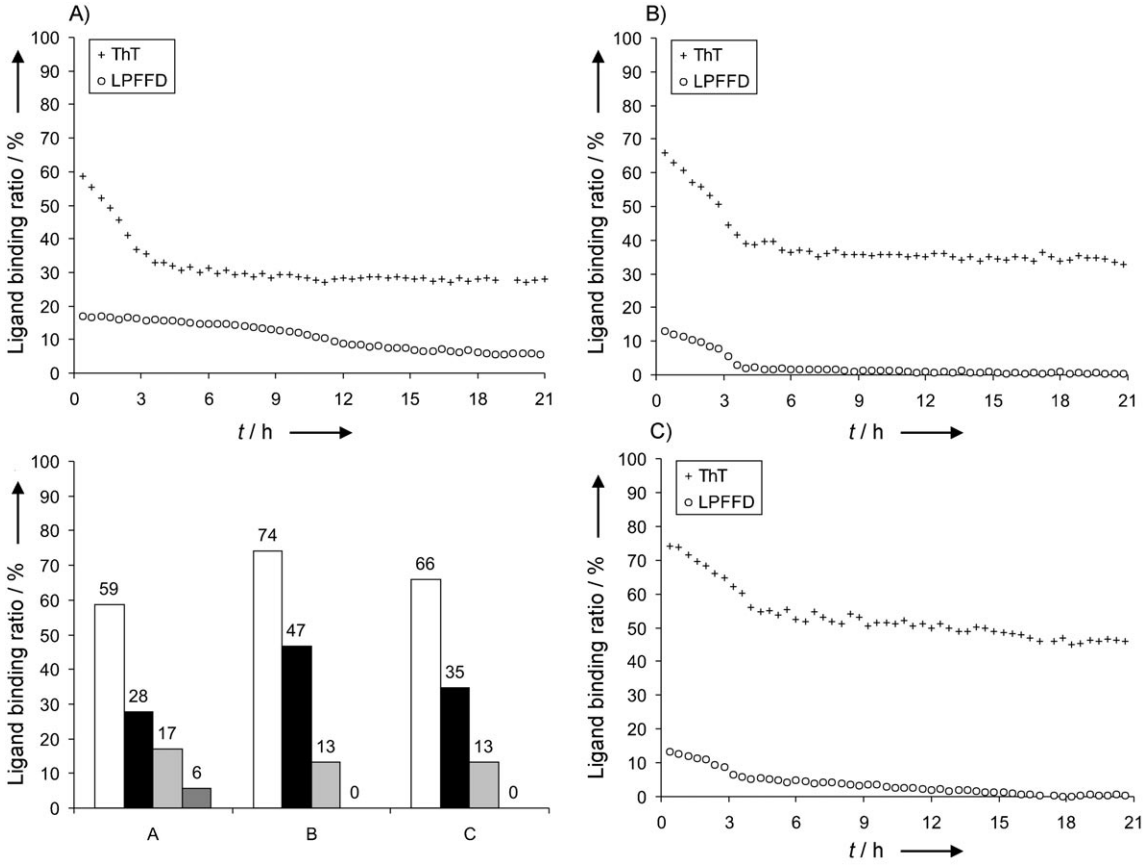

Figure 2. Time-dependence of the bound fraction after sample preparation in phosphate buffer (10 mM, pH 7.4) without NaCl for ThT: +, and LPFFD: ○. Concentrations were 100 μM for Aβ(1–42) and 500 μM for the ligands. A) Bound fractions in single ligand experiments. B) Double ligand experiment with LPFFD as the first and ThT as the second ligand. C) Double ligand experiment with ThT as the first and LPFFD as the second ligand. The column diagram displays the initial and the final values of the bound fraction for ThT and LPFFD: white (ThT, 0 h); black (ThT, 24 h); light gray (LPFFD, 0 h); dark gray (LPFFD, 24 h). For ThT, the slopes that are fitted for the first 4 h are −7.75, −7.56 and −4.89%/h on panels A, B and C, repectively. For LPFFD, the slopes fitted for the first 4 h are −0.38, −3.10 and −2.40%/h on panels A, B and C, repectively.

the samples after the 24 h observation period, we tested the behavior of the mixtures in the NMR spectroscopic binding experiments for another 24 h after agitation of the samples. For the ThT–Aβ(1–42) mixture, the ThT-bound fraction was initially higher at 69%, which had declined to 45% after an additional 24 h of observation (Figure 3A). The LPFFD–Aβ(1–42) system exhibited a constant binding ratio of 6%, which is identical to the value that was measured before shake-up (Figure 3A). Samples B and C exhibited practically the same behavior: 1) initial ThT-bound fractions of around 70%, which slowly decreased to ca. 60%; and 2) an initial binding ratios of 10% for LPFFD, which fell to zero at the same relative rate as for ThT (Figure 3B and C). These results strongly suggested that the sedimentation and flocculation of the Aβ(1–42) assemblies are responsible for the decay of the apparent bound fraction.

It is known from the methodology of the affinity chromatography that elevated salt concentrations (100–1000 mM) can destroy protein–ligand complexes and thereby have an eluting effect.[55] To make use of the media with increased salt concentration, and to gain information on our system in a biologically more relevant medium, the binding experiments were carried out for LPFFD and ThT in a phosphate buffer that contained NaCl in physiological concentration (PBS, 130 mM NaCl). The bound fractions did not exhibit transient behavior and their levels are in line with the equilibrium values that were obtained in phosphate buffer (Figure 4). This can be explained by the absence of weak binding that is caused by the elevated salt concentration. This finding indicates that the NMR spectroscopy experiment is extremely sensitive to the weak interactions, and has high on/off rates, which effectively destroy the NMR signals. For samples that were prepared in phosphate buffer without NaCl, these weak interactions were removed from the detection volume of the NMR probe head by the sedimentation processes.

The proven effect of the sedimentation on the NMR signals underlined the importance of particle size measurements under the same conditions as in the binding tests. It should be noted that under the measurement conditions applied, no resonance of oligomer or monomer-sized Aβ(1–42) ($M_W < 60$–100 kDa), which would have resulted from possible disaggregation of the fibrils was detected by NMR spectroscopy.

Particle size changes monitored by diffuse light-scattering measurements

In accordance with the theory of static multiple light scattering,[56] the diffuse back-scattering decreases with increasing particle size (e.g., caused by flocculation) when the particle

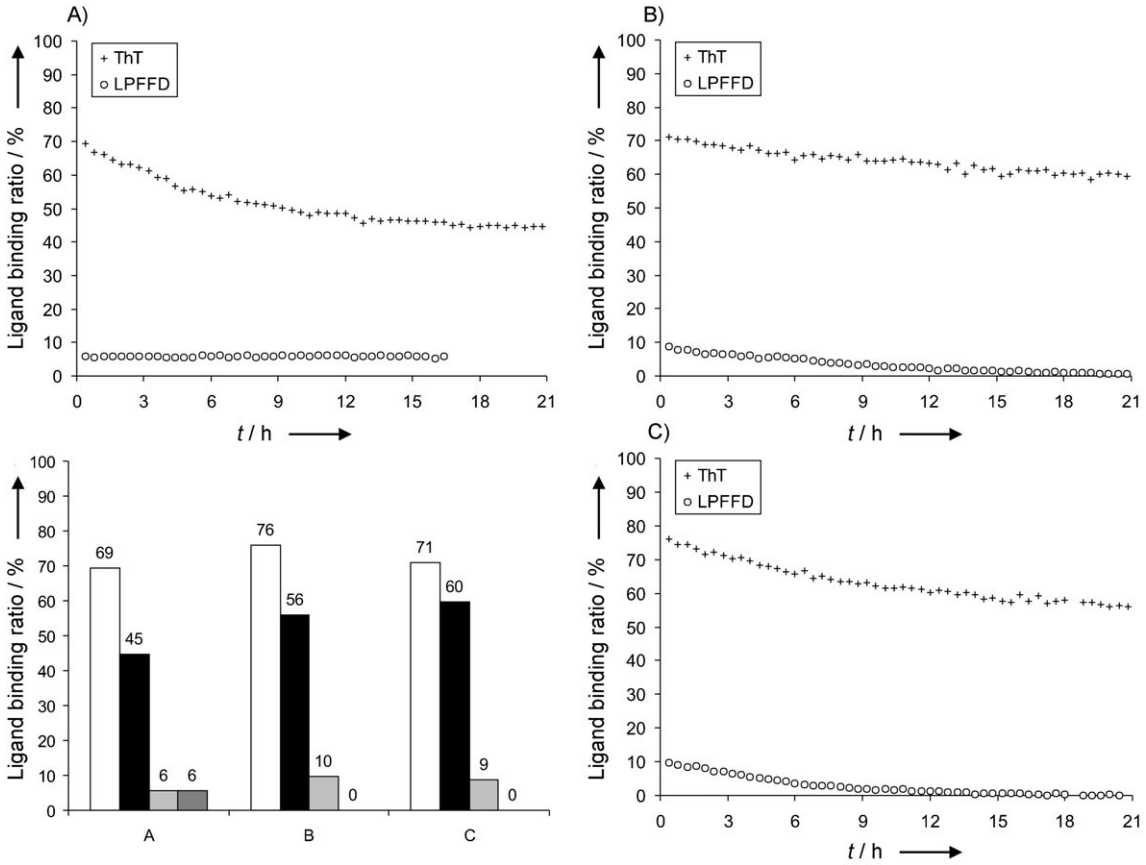

Figure 3. Time-dependence of the bound fraction after resuspending the samples in phosphate buffer (10 mM, pH 7.4) without NaCl for ThT: +, and LPFFD: ○ Concentrations were 100 μM for Aβ(1–42) and 500 μM for the ligands. A) bound fractions in single ligand experiments. B) Double ligand experiment with LPFFD as the first and ThT as the second ligand. C) Double ligand experiment with ThT as the first and LPFFD as the second ligand. The column diagram displays the initial and the final values of the bound fraction for ThT and LPFFD: white (ThT, 0 h); black (ThT, 24 h); light gray (LPFFD, 0 h); dark gray (LPFFD, 24 h).

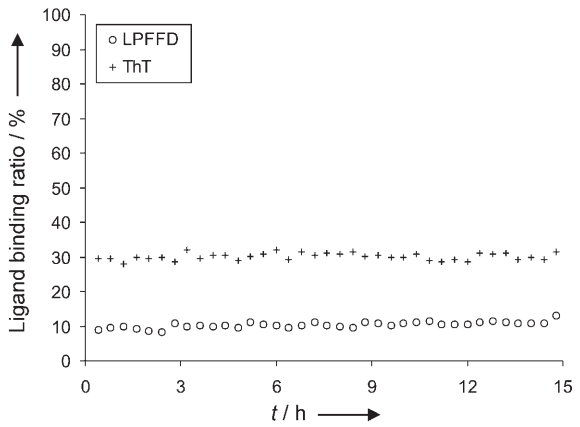

Figure 4. Time dependence of the bound fraction after sample preparation in phosphate buffer (10 mM, pH 7.4) with 130 mM NaCl (PBS) for ThT–Aβ(1–42): +, and LPFFD–Aβ(1–42): ○. Concentrations were 100 μM for Aβ(1–42) and 500 μM for the ligands.

diameter exceeds 0.3 μm. The particle migration phenomena (e.g., sedimentation) induces particle volume fraction changes at the extremities of the sample. A higher volume fraction increases the back-scattered light intensity. In our study, the time-dependent changes in the back-scattered light intensity were monitored photographically. To follow the flocculation and sedimentation processes, BS(t,z), the back-scattering intensity profile was plotted against sample height and time.[57–59]

For pure fibrillar Aβ(1–42), slow sedimentation was revealed by the changes in the BS intensity profile (Figure 5A). For the LPFFD–Aβ(1–42) sample (the same composition as was used in the NMR spectroscopic binding test), the BS intensity dropped uniformly along the full length of the sample; this indicates a flocculation phenomenon that is induced by the peptide ligand (Figure 5B). The spikes in the BS intensity that were obtained after 3 h are related to the precipitated material attached to the test tube wall. The fully flocculated state was reached after 24 h, where the BS baseline was at around 50 BS intensity units.

For the freshly prepared ThT–Aβ(1–42) sample (the same composition as used in the NMR spectroscopic binding test), the results are given in Figure 5C. During the first 3 h, a steep BS intensity fall was observed over the whole height of the sample, which indicated a significant particle size increase due to flocculation. The final low BS intensity was attained after 3 h, and the fluctuation in the BS intensity revealed that large sediments were stuck to the tube wall, which was otherwise easily seen in the original images (Figure S3). These findings pointed to a rapid ThT-induced self-association of the fibrillar Aβ(1–42). The timescale of the particle size changes corresponded closely to the binding ratio decrease that was observed in the NMR spectroscopy experiments.

Diffuse light scattering measurements were performed in PBS, for the pure Aβ(1–42) fibrils and the LPFFD–Aβ(1–42) samples. The elevated salt concentration increased the tendency of the Aβ(1–42) fibrils to flocculate (Figure 6A). On the other hand, the effect of LPFFD was still observable; the decrease in the BS intensity change was faster than the pure Aβ(1–42) fibrils (Figure 6B).

Particle size and morphology changes monitored by TEM measurements

The effects of LPFFD and ThT on the process of fibrillar Aβ(1–42) assembly was investigated by using negative staining. To facilitate direct comparison, samples were prepared with the same protocol as used for the NMR measurements. As a control experiment, fibrillar Aβ(1–42) was incubated in 10 mM phosphate buffer at pH 7.4 without NaCl for 24 h. Only

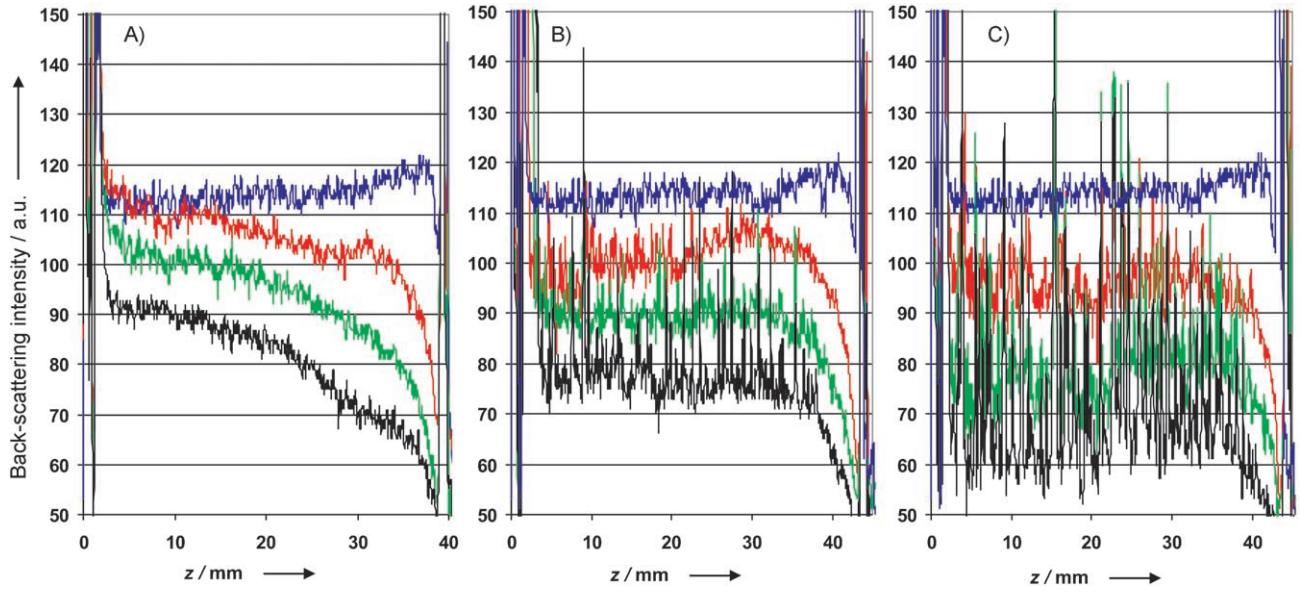

Figure 5. Diffuse light-scattering results obtained on freshly prepared samples of fibrillar Aβ(1–42) (A), LPFFD–Aβ(1–42) (B) and ThT–Aβ(1–42) (C); measured at $t = 0$ (blue), 1 (red), 2 (green) and 3 h (black). The samples were prepared in phosphate buffer (10 mM, pH 7.4) without NaCl. Concentrations were 100 μM for Aβ(1–42) and 500 μM for the ligands.

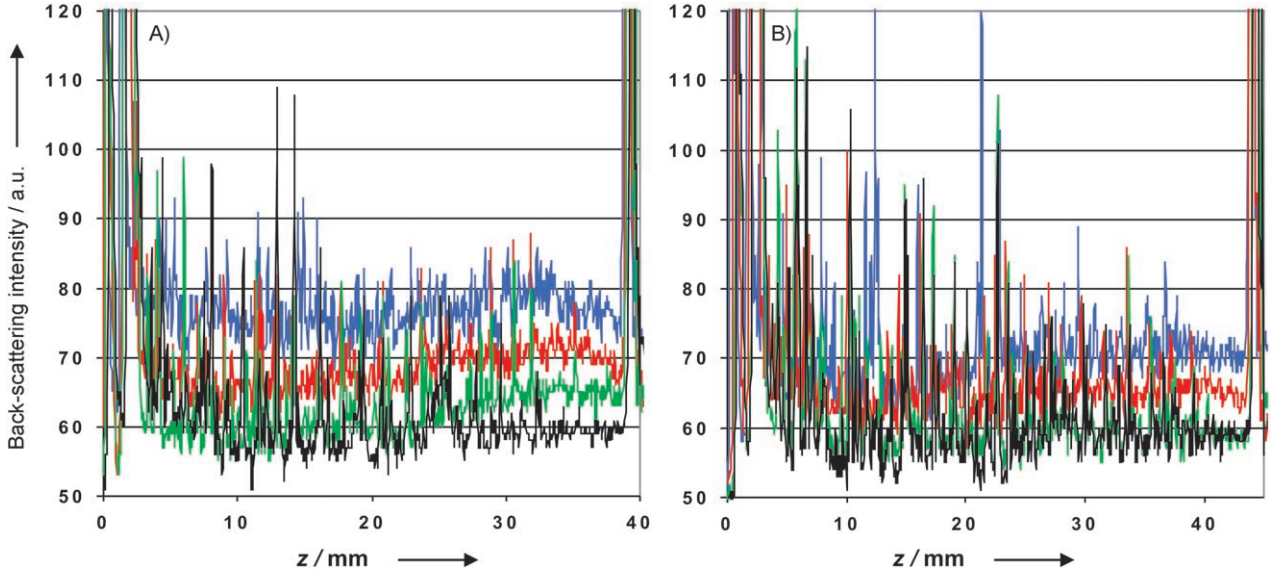

Figure 6. Diffuse light scattering results obtained on freshly prepared samples of fibrillar Aβ(1–42) (A) and LPFFD–Aβ(1–42) (B); measured at $t = 0$ (blue), 1 (red), 6 (green) and 24 h (black). The samples were prepared in phosphate buffer (pH 7.4) with 130 mM NaCl (PBS). Concentrations were 100 μM for Aβ(1–42) and 500 μM for the ligands.

separate (nonflocculated) mature fibrils were observed during the studied 24 h (Figure 7A, A1 and A2). The large floccules of Aβ(1–42) fibrils appeared even in the first images that were taken after the sample preparation for the LPFFD–Aβ(1–42) mixture (Figure 7A, B1), which is in agreement with the light-scattering results. Later, at 3 h (Figure 7A, B), the samples displayed a further increase in particle size, and the original morphology of the fibrils could hardly be observed. For images recorded after 24 h, see the Supporting Information.

Addition of a five-fold excess of ThT to the fibrillar Aβ(1–42) resulted in large interfibrillar assemblies (Figure 7B, C1 and C2). The mature fibrils started to adhere closely together immediately after the addition of ThT (Figure 7B, C1). After 3 h, large particles were formed by the flocculated fibrils (Figure 7B, C2). By the end of the 24 h observation period, no particles could be detected on the TEM grid. Because a significant particle size increase could be unequivocally detected with the light-scattering experiment, we believe that the large floccules could not be captured by the TEM methodology applied.

When LPFFD was added first to the fibrillar Aβ(1–42), and then ThT, even larger interfibrillar assemblies were seen on the first TEM images (Figure 7B, D1). Later, the adhesion of the extraordinarily large particles to the TEM grid could not be achieved even after incubation for 3 h.

TEM experiments were performed in PBS for the pure Aβ(1–42) fibrils and the LPFFD–Aβ(1–42) samples. In accordance with the diffuse light scattering results, some fibrils were attached to each other even at the first measurement point in the pure Aβ(1–42) in PBS sample (Figure 8, A1), and the flocculation became extensive after 6 h (Figure 8, A2). Addition of LPFFD to the system resulted in a significant particle size increase even at 0 h (Figure 8, B1). After 6 h, a large network of attached fibrils was observable (Figure 8, B2).

Time-dependent ζ-potential measurements

It is known from the DLVO theory[60,61] that a charged particle surface can efficiently inhibit flocculation via the electrostatic repulsion between the double layers of counterions surrounding the interacting particles. The electrostatic stabilizing effect can be measured through the ζ-potential (electrokinetic potential), which is the electric potential that exists at the interface between the hydrated particle and the bulk solution. It is widely accepted that if the absolute value of the ζ-potential is below 30 mV, a dispersed system is susceptible to flocculation. The ζ-potential of the fibrillar Aβ(1–42) was around −16 mV and did not change appreciably during the observation period of 24 h (Figure 9). Upon the addition of LPFFD to the fibrillar Aβ(1–42), the initial value of the ζ-potential was the same as was observed for pure Aβ(1–42), but it slowly decreased with time and reached a value of −20 mV. For samples that contained ThT, the decay of the ζ-potentials was more pronounced, with a final value of −23 mV. The measurement in PBS resulted in similar behavior.

Discussion

A NMR spectroscopic binding experiment is capable of monitoring weak binding of neuroprotective molecules to Aβ aggregates

NMR spectroscopic binding experiments are based on the fact that ^{1}H nuclei in large proteins (above 60–100 kD, depending on the shape) exhibit extremely fast transversal relaxation in the solution phase due to the slow rotational tumbling. Hence, these particles do not generate detectable NMR signals. Small molecules that are rapidly tumbling in solution, such as the studied short peptide ligands and ThT, furnish narrow resonances with intensities that are proportional to the concentration

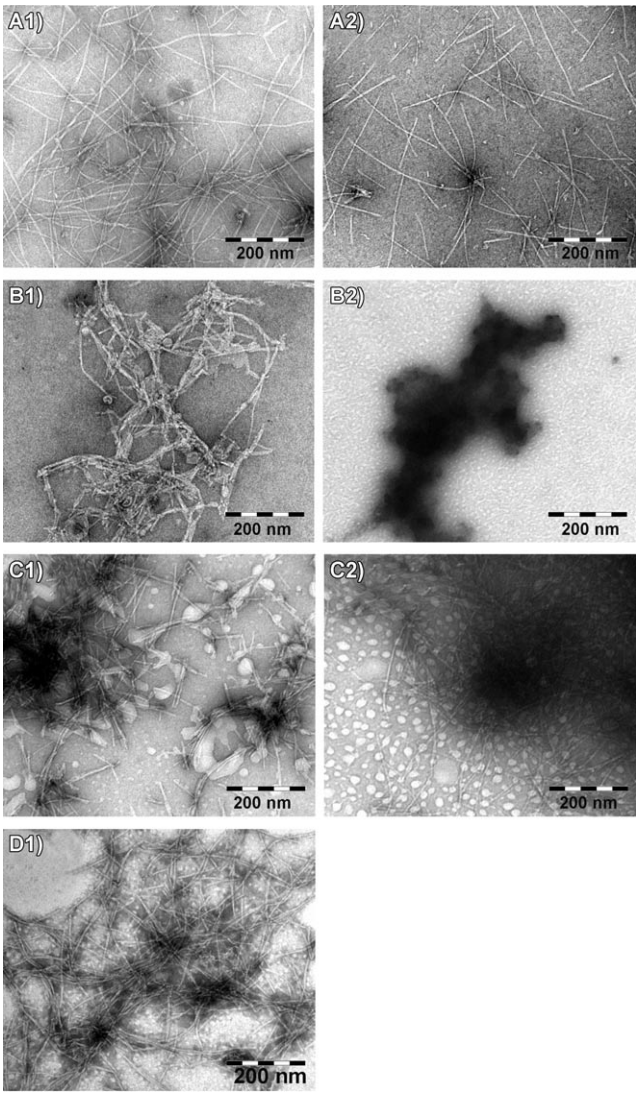

Figure 7. A) TEM images that indicate the effects of LPFFD on the flocculation process for fibrillar Aβ(1–42): for pure fibrillar Aβ(1–42) sampled at $t=0$ (A1), and 3 h (A2) and for LPFFD–Aβ(1–42) sampled at $t=0$ (B1), 3 h (B2). The samples were prepared in phosphate buffer (10 mM, pH 7.4) without NaCl. B) the TEM images indicate the effects of ThT on the flocculation process for fibrillar Aβ(1–42): for ThT–Aβ(1–42) sampled at $t=0$ (C1) and 3 h (C2) and for LPFFD–ThT–Aβ(1–42) sampled at t = 0 h (D1). The samples were prepared in phosphate buffer (10 mM, pH 7.4) without NaCl.

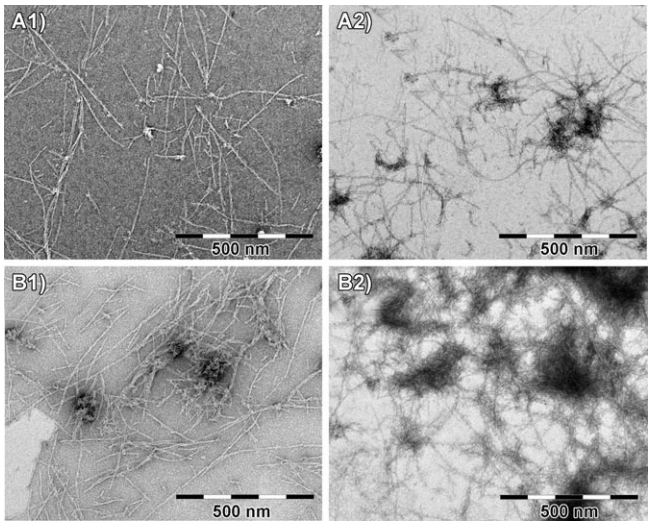

Figure 8. TEM images that indicate the effects of LPFFD on the flocculation process for fibrillar Aβ(1–42): for pure fibrillar Aβ(1–42) sampled at $t=0$ (A1), and 6 h (A2) and for LPFFD–Aβ(1–42) sampled at $t=0$ (B1), 6 h (B2). The samples were prepared in phosphate buffer (10 mM, pH 7.4) with 130 mM NaCl (PBS).

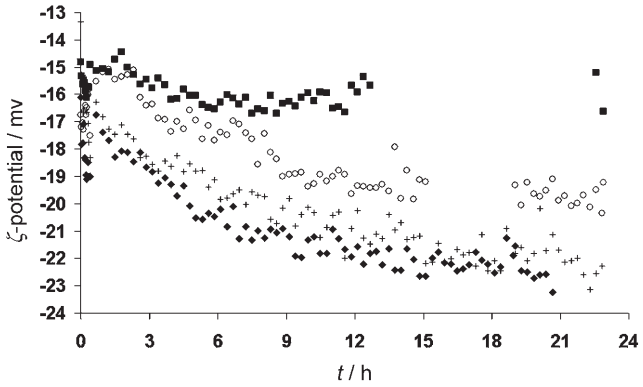

Figure 9. Time-dependent ζ-potential measurements: ■ pure Aβ(1–42); + ThT–Aβ(1–42); ○ LPFFD–Aβ(1–42); ● LPFFD–ThT–Aβ(1–42). The samples were prepared in phosphate buffer (10 mM, pH 7.4) without NaCl. Concentrations were 100 μM for Aβ(1–42) and 500 μM for the ligands.

of the free ligand. When a small molecule is bound to a large macromolecule, its resonances are destroyed by the fast relaxation, and thus the measured peak intensities decrease with the bound fraction. As reported for fibrillar Aβ(14–23),[52] peptide ligands exhibit decreased signal intensities upon binding to large Aβ(14–23) aggregates. Our results revealed that the methodology is capable of monitoring ligand binding to the large Aβ(1–42) fibrils that are otherwise invisible to solution NMR spectroscopy. Among the advantages of the technique are the facts that the measurements are carried out on native Aβ(1–42) fibrils (a fluorescence tag or a linkage to a solid support is unnecessary) and under the same conditions (ligand and target concentrations, pH and ionic strength) as in the biological tests.

The observed signal quenching reveals the binding of the short neuroprotective peptides to the fibrillar Aβ(1–42), which indicates that the immediate binding to the Aβ(1–42) fibrils can play an important role in their short timeframe protective effect.

Complex time-dependent binding behavior is caused by ligand-induced changes in the sedimentation rate of Aβ(1–42)

The NMR resonance quenching is very sensitive to weak binding, which effectively destroys ligand signals in the detection volume of the NMR probe head. For sedimenting systems such as the Aβ(1–42) fibrils in aqueous medium, these weak interactions are relocated to the bottom of the test tube, thereby resulting in a lower apparent bound fraction in the equilibrium. Time-dependent binding measurements unequivocally demonstrated that the binding phenomena are transient in the first

3 h and 12 h for ThT and LPFFD, respectively. The decreasing binding ratios lend support to the view that multiple binding sites exist for a single ligand,[39] and it is very likely that ligands induce particle size changes, thereby causing faster sedimentation and removal of the weak ligand–fibril interactions from the NMR detection volume. Upon addition of NaCl in physiological concentration, its eluting effect eliminated the weak interactions, thus, the transient binding behavior disappeared. In this case, the strongly bound fraction of the ligand was observed.

The double ligand experiments yielded highly intriguing results: 1) when the peptide is added first, ThT can not fully and immediately replace the peptide ligand; 2) the replacement is complete after several hours; 3) when ThT is added first, it cannot prevent the weak binding of LPFFD, but the extent of peptide binding decreases with the rate of decline of ThT binding; 4) LPFFD does not decrease the extent of the NMR spectroscopy-detected ThT binding, and moreover, the quantity of the bound ThT is always higher when LPFFD is present; and 5) no solution NMR spectroscopically visible monomeric or oligomeric Aβ(1–42) signal accompanies the resonances of the studied ligands in the spectra. Quantitative analysis of the first 4 h of the curves reveals that the decay can be best fitted with a linear equation, however, a curvature can be detected; this indicates slightly increasing slopes. This finding supports the sedimentation hypothesis. The decay rate is always higher when ThT is present, which correlates well with the results of the particle size measurements; ThT induces faster flocculation with larger particle sizes than LPFFD.

If a multiple binding site model that involves a partial overlap between the different types of ligands is considered, then fast equilibration of the bound fractions should be observed, and the results should be independent of the sample preparation sequence and time. Hence, these findings cannot be explained in the simplified framework of a multiple binding site model where the ligands are competing on the constant surface of the Aβ(1–42) fibrils. It appears probable that ligand-induced structural changes that affect the binding sites on Aβ-(1–42) can account for the complex time-dependent replacement behavior.

LPFFD did not decrease NMR spectroscopy-detected ThT binding

LPFFD did not decrease the extent of NMR spectroscopopy-detected ThT binding but rather increased it, and resonances that are attributable to monomeric/oligomeric Aβ(1–42) could not be detected in the NMR spectra, which renders disaggregation unlikely under the conditions applied. This is supported by literature results that indicate that Aβ(17–21) analogues are able to promote the inter-protofibrillar association.[62,63] In order to test the utility of this concept for fibrillar Aβ(1–42), particle size measurements were carried out.

Both LPFFD and ThT causes flocculation of the Aβ aggregates

The results of diffuse light scattering experiments strongly suggest a significant time-dependent increase in the particle size in both phosphate buffer and PBS, and the rate correlates very well with the change in the bound fraction in the NMR spectroscopy experiments. The TEM images corroborate these observations because interfibrillar association can be clearly observed even within 10 min of mixing the fibrillar Aβ(1–42) samples with either LPFFD or ThT. In light of the rapid occurrence of ligand-induced interfibrillar association, the slow kinetics of the LPFFD–ThT replacement experiment can be adequately explained. Despite the millimolar binding, LPFFD makes the Aβ-(1–42) fibrils susceptible to flocculation; this leads to intercalated ligands, which in turn decreases the dissociation rate and thereby hinders the replacement by ThT. The intercalation process might be of relevance in regard to the β-sheet-breaking effect of short peptides too, which can occur after a few days of coincubation under specific conditions.[1]

When ThT is added first, only nonspecific surface adsorption is possible for LPFFD, which cannot significantly affect the flocculation and the higher-order structure that is generated by ThT. It is more difficult to explain why the β-sheet-breaker peptide increased the ThT binding to the Aβ(1–42). We speculate that the bound peptide can expose an increased number of binding sites for ThT, thus the ThT binds to the Aβ-bound peptide as a second layer.

Flocculation is a result of noncovalent crosslinking

In order to gain information on the driving force of the flocculation process, we carried out ζ-potential measurements. These indicated that the studied ligands do not decrease the absolute value of the ζ-potential of the fibrillar Aβ(1–42), which suggests that the interfibrillar association is not simply electrostatically driven, but that specific noncovalent cross-linking interactions are responsible for the phenomenon. Interestingly, the ζ-potential values become even more negative after ligand binding.

Conclusions

Observations in this work revealed short time-domain structural changes that are caused by the interactions of the studied ligands with the Aβ(1–42) fibrils; these interactions might have implications for the neuroprotective effect that is exerted by these ligands (Figure 10). First, after rapid ligand binding, floccules are formed, which can result in a considerable decrease in specific surface area, and a lower concentration for the mobile fibrillar Aβ(1–42) particles. Because the mechanistic hypotheses of the Aβ toxicity assume that the surface of the fibrils is accessible for the cell-membrane-bound receptors, a decreased specific surface area of Aβ can obviously lead to a decreased toxicity. Besides the increased susceptibility to flocculation, the studied ligands partially cover the otherwise mobile Aβ fraction, which causes a further decrease in the accessible

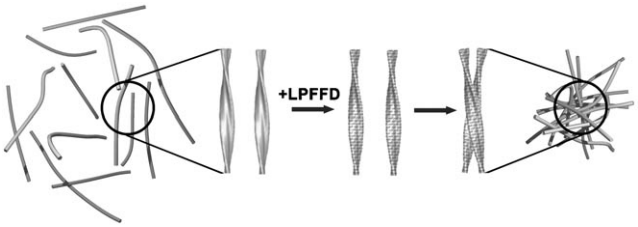

Figure 10. Schematic representation of the ligand-induced flocculation (the fibril model is taken from ref. [43]).

surface. Second, an increase was observed in the absolute value of the ζ-potential in the negative region, a phenomenon which might partially prevent the interaction of Aβ with negatively charged cell membrane features.

In conclusion, we propose that small molecules and peptides/peptidomimetics can have crucial effects on the higher-order structure of Aβ in a shorter time-domain than that in which the β-sheet-breaking effect appears, and this has implications for their protective effect. These findings also contribute to a better understanding of the molecular mechanism of the β-sheet-breaking effect.

Experimental Section

Preparation of fibrillar Aβ(1–42): Aβ(1–42) was synthetized as reported earlier.[64] Protected amino acids and coupling reagents were obtained from Orpegen Pharma (Heidelberg, Germany), and solvents were obtained from Sigma–Aldrich. All chemicals were used without additional purification.

For the preparation of purely fibrillar samples, purified Aβ(1–42) was dissolved in hexafluoroisopropanol (HFIP) and incubated overnight at ambient temperature. After removal of the organic solvent in vacuo, the peptide was dissolved in 0.5% aqueous NaN_3 solution (*w/v*) to a concentration of 500 μg mL^{-1}, seeded with a definite volume of pre-aggregated Aβ(1–42) solution ($c = 0.5$ mg mL^{-1}, in 1:50 volume ratio), sonicated for 10 min and incubated at 37 °C for 3 days. In order to remove the large, flocculated aggregates of Aβ-(1–42), the stock solution was centrifuged at 1000 *g* for 1 min. The supernatant (which exhibited only a slight opacity) was then transferred into test tubes and centrifuged at 15000 *g* and 4 °C for 30 min. The pellets were collected, washed twice by resuspending them in deionized water, then centrifuged under the same conditions as before. Finally, the pellets were suspended in smaller amount of deionized water so that the concentration of this stock solution was 775 μM, as determined by a bicinchoninic acid protein assay by following the standard Sigma–Aldrich protocol. Aliquots were transferred into test tubes, frozen with liquid N_2 at −196 °C and stored at −30 °C. With this methodology, the sample preparation could be standardized, whereby the samples contained exclusively mature Aβ(1–42) fibrils in the same concentration and aggregation grade.

Synthesis of short neuroprotective peptides: LPFFD, LPYFD-NH_2, FRHDS-NH_2, GGGGG-NH_2 and RIIGL-NH_2 were synthetized in the solid phase by using Boc chemistry. The pentapeptides were purified by preparative RP-HPLC and their purities were checked by ESI-MS.

TEM experiments. Droplets of solutions (10 μL) were placed onto carbon-film-coated 400-mesh copper grids (Electron Microscopy Sciences, Washington DC, USA). The solution of the aggregated sample was applied to the grid and incubated for 2 min. The specimen was then fixed with 0.5% glutaraldehyde solution (*v/v*) for 1 min, washed three times with deionized water, and finally stained with 2% uranyl acetate (*w/v*) by incubating for 2 min. Excess solution was removed by suction with a filter paper. Specimens were studied with a Philips CM 10 transmission electron microscope (FEI Company, Hillsboro, Oregon, USA) that was operating at 100 kV. Images were taken with a Megaview II Soft Imaging System routinely at magnifications of 25000× and 46000×, and analyzed with an AnalySis® 3.2 software package (Soft Imaging System GmbH, Münster, Germany).

NMR spectroscopy sample preparation: Stock solutions (5 mM) of ligands were prepared in phosphate D_2O buffer (10 mM, pH 7.4). First, ligand stock solution (15 μL) and buffer (120 μL) were mixed and transferred to a 2.5 mm capillary NMR tube, and the reference ^{1}H NMR spectrum was recorded. Subsequently, fibrillar Aβ stock solution (20 μL) was transferred into the NMR tube and the mixture was sonicated for 5 s to facilitate proper mixing. In the final sample, the ligand/fibrillar Aβ(1–42) ratio was 5:1. For the competition measurements, the second ligand was added as a stock solution (15 μL) to the existing sample after coincubation with the first ligand for 50 min (if not mentioned otherwise). For the experiments that were carried out in PBS, the phosphate D_2O buffer contained NaCl (130 mM).

NMR spectroscopic binding test: The quantitative NMR spectroscopic binding test was performed in four steps: 1) the reference spectrum of the free ligand was recorded; 2) the second spectrum was run after the addition of Aβ stock solution and thermal equilibration in the NMR spectrometer for 30 min; 3) the reference spectrum was scaled to the small concentration difference due to dilution; and 4) the difference spectrum was calculated and integrated, and its ratio was compared to the reference intensities to give the bound fraction of the ligand.

All NMR spectra were recorded on a Bruker AV600 spectrometer that was equipped with a 2.5 mm triple-resonance capillary probe at 25 °C. The ^{1}H NMR spectroscopy measurements were performed with a WATERGATE[65] solvent suppression scheme. All samples were measured with the same experimental parameters, the same spectrometer and the same probe. For the relaxation delay, 2 s was used; the delay for binomial water suppression was 150 μs; the number of scans was 256. One measurement took 24 min of experiment time (with dummy scans).

Saturation transfer difference (STD)[66] measurements were performed with the WATERGATE water suppression pulse scheme. The irradiation power was 20 Hz, which was applied on-resonance at 0 ppm and off-resonance at 40 ppm. A total of 2024 scans were accumulated for each pseudo-2D experiment, which resulted in a total experiment time of 8 h.

All NMR spectra were processed and analyzed with Topspin 2.0 (Bruker) in such a way that line-width effects on the intensity of the signal were negligible. Extreme care was taken to scale the measured signal intensities properly with respect to the slightly different concentrations in the reference spectra and the final Aβ-containing samples. All the measurements were repeated at least three times on separate samples, and the reproducibility of the bound fractions were within the relative error of 2%.

Diffuse light-scattering experiments. All photos were taken with a Canon EOS 20D with a Tamron 28–75/2.8 objective. The shutter speed was 1/200, the aperture was 1/16, and the focal distance

was 75 mm. Images were analyzed with ImageTool 3.0 software (University of Texas Health Science Center at San Antonio, Texas).

ζ-Potential measurements. All experiments were performed at 25 °C with a Malvern Zetasizer Nano ZS instrument (Malvern Instruments Ltd. Worcestershire, UK) equipped with a He–Ne laser (633 nm), laser Doppler electrophoresis being combined with phase analysis light scattering (M3-PALS® technology).

Acknowledgements

This work was performed in the Szeged Neurobiological Knowledge Center, and was supported by grant RET 08/2004. T.A.M. acknowledges the award of a János Bolyai scholarship from the Hungarian Academy of Sciences and grant OTKA-NF69316. L.F. acknowledges postdoctoral grant KPÖ0040/2006 from the Hungarian Ministry of Education.

Keywords: beta-amyloid peptides · electron microscopy · neurochemistry · NMR spectroscopy

[1] S. Bieler, C. Soto, *Curr. Drug. Targets* **2004**, *5*, 553–558.
[2] J-P. Brion, *Eur. Neurol.* **1998**, *40*, 130–140.
[3] M. Blurton-Jones, F. M. Laferla, *Curr. Alzheimer Res.* **2006**, *3*, 437–448.
[4] B. Clippingdale, J. D. Wade, C. J. Barrow, *J. Pept. Sci.* **2001**, *7*, 227–249.
[5] P. T. Lansbury, H. A. Lashuel, *Nature* **2006**, *443*, 774–779.
[6] T. A. Bayer, O. Wirths, K. Majtenyi, T. Hartmann, G. Multhaup, K. Beyreuther, C. Czech, *Brain Pathol.* **2001**, *11*, 1–11.
[7] K. N. Dahlgren, A. M. Manelli, W. B. Stine, L. K. Baker, G. A. Krafft, M. J. LaDu, *J. Biol. Chem.* **2002**, *277*, 32046–32053.
[8] Z. Datki, R. Papp, D. Zádori, K. Soós, L. Fülöp, A. Juhász, G. Laskay, C. Hetényi, E. Mihalik, M. Zarándi, B. Penke, *Neurobiol. Dis.* **2004**, *17*, 507–515.
[9] Z. Datki, A. Juhász, M. Gálfi, K. Soós, R. Papp, D. Zádori, B. Penke, *Brain Res. Bull.* **2003**, *62*, 223–229.
[10] C. Adessi, C. Soto, *Drug Dev. Res.* **2002**, *56*, 184–193.
[11] J. Hardy, *Proc. Natl. Acad. Sci. USA* **1997**, *94*, 2095–2097.
[12] J. Hardy, D. J. Selkoe, *Science* **2002**, *297*, 353–356.
[13] M. A. Findeis, *Biochim. Biophys. Acta Mol. Basis Dis.* **2000**, *1502*, 76–84.
[14] F. E. Cohen, J. W. Kelly, *Nature* **2003**, *426*, 905–909.
[15] J. E. Gestwicki, G. R. Crabtree, I. A. Graef, *Science* **2004**, *306*, 865–869.
[16] T. Wyss-Coray, C. Lin, F. R. Yan, G. Q. Yu, M. Rohde, L. McConlogue, E. Masliah, L. Mucke, *Nat. Med.* **2001**, *7*, 612–618.
[17] D. J. Selkoe, *Ann. Intern. Med.* **2004**, *140*, 627–638.
[18] E. M. Snyder, Y. Nong, C. G. Almeida, S. Paul, T. Moran, E. Y. Choi, A. C. Nairn, M. W. Salter, P. J. Lombroso, G. K. Gouras, P. Greengard, *Nat. Neurosci.* **2005**, *8*, 1051–1058.
[19] J. P. Tyszkiewicz, Z. Yan, *J. Neurophysiol.* **2005**, *93*, 3102–3111.
[20] D. M. Walsh, I. Klyubin, J. V. Fadeeva, W. K. Cullen, R. Anwyl, M. S. Wolfe, M. J. Rowan, D. J. Selkoe, *Nature* **2002**, *416*, 535–539.
[21] J. P. Cleary, D. M. Walsh, J. J. Hofmeister, G. M. Shankar, M. A. Kuskowski, D. J. Selkoe, K. H. Ashe, *Nat. Neurosci.* **2005**, *8*, 79–84.
[22] A. Deshpande, E. Mina, C. Glabe, J. Busciglio, *J. Neurosci.* **2006**, *26*, 6011–6018.
[23] M. Isaacs, D. B. Senn, M. L. Yuan, J. P. Shine, B. A. Yankner, *J. Biol. Chem.* **2006**, *281*, 27916–27923.
[24] O. Butovsky, A. E. Talpalar, K. Ben-Yaakov, M. Schwartz, *Mol. Cell. Neurosci.* **2005**, *29*, 381–393.
[25] M. Rapoport, H. N. Dawson, L. I. Binder, M. P. A. Vitek, Ferreira, *Proc. Natl. Acad. Sci. USA* **2002**, *99*, 6364–6369.
[26] V. Szegedi, G. Juhasz, D. Budai, B. Penke, *Brain Res.* **2005**, *1062*, 120–126.
[27] G. Chen, K. S. Chen, J. Knox, J. Inglis, A. Bernard, S. J. Martin, A. Justice, L. McConlogue, D. Games, S. B. Freedman, R. G. M. Morris, *Nature* **2000**, *408*, 975–979.
[28] T. Sato, P. Kienlen-Campard, M. Ahmed, W. Liu, H. L. Li, J. I. Elliott, S. Aimoto, S. N. Constantinescu, J. N. Octave, S. O. Smith, *Biochemistry* **2006**, *45*, 5503–5516.
[29] C. Soto, M. S. Kindy, M. Baumann, B. Frangione, *Biochem. Biophys. Res. Commun.* **1996**, *226*, 672–680.
[30] C. Adessi, C. Soto, *Drug. Dev. Res.* **2002**, *56*, 184–193.
[31] C. Hilbich, B. Kisterswoike, J. Reed, C. L. Masters, K. Beyreuther, *J. Mol. Biol.* **1992**, *228*, 460–473.
[32] C. Soto, E. M. Castano, R. A. Kumar, R. C. Beavis, B. Frangione, *Neurosci. Lett.* **1995**, *200*, 105–108.
[33] L. O. Tjernberg, J. Näslund, F. Lindqvist, J. Johansson, A. R. Karlström, J. Thyberg, L. Terenius, C. Nordstedt, *J. Biol. Chem.* **1996**, *271*, 8545–8548.
[34] S. Narayanan, B. Reif, *Biochemistry* **2005**, *44*, 1444–1452.
[35] V. Szegedi, L. Fülöp, T. Farkas, E. Rózsa, H. Robotka, Z. Kis, Z. Penke, S. Horváth, Z. Molnár, Z. Datki, K. Soós, J. Toldi, D. Budai, M. Zarándi, B. Penke, *Neurobiol. Dis.* **2005**, *18*, 499–508.
[36] L. Fülöp, M. Zarándi, Z. Datki, K. Soós, B. Penke, *Biochem. Biophys. Res. Commun.* **2004**, *324*, 64–69.
[37] P. Inbar, J. Yang, *Bioorg. Med. Chem. Lett.* **2006**, *16*, 1076–1079.
[38] H. LeVine, *Arch. Biochem. Biophys.* **1997**, *342*, 306–316.
[39] H. LeVine, *Amyloid* **2005**, *12*, 5–14.
[40] T. Lührs, C. Ritter, M. Adrian, D. Riek-Loher, B. Bohrmann, H. Döbeli, D. Schubert, R. Riek, *Proc. Natl. Acad. Sci. USA* **2005**, *102*, 17342–17347.
[41] R. Tycko, *Curr. Opin. Struct. Biol.* **2004**, *14*, 96–103.
[42] C. Ritter, M. L. Maddelein, A. B. Siemer, T. Luhrs, M. Ernst, B. H. Meier, S. J. Saupe, R. Riek, *Nature* **2005**, *435*, 844–848.
[43] C. Sachse, C. Xu, K. Wieligmann, S. Diekmann, N. Grigorieff, M. Fändrich, *J. Mol. Biol.* **2006**, *362*, 347–354.
[44] H. LeVine, *Protein Sci.* **1993**, *2*, 404–410.
[45] H. Naiki, K. Higuchi, M. Hosokawa, T. Takeda, *Anal. Biochem.* **1989**, *177*, 244–249.
[46] H. Naiki, K. Higuchi, K. Matsushima, A. Shimada, W. H. Chen, M. Hosokawa, T. Takeda, *Lab. Invest.* **1990**, *62*, 768–773.
[47] H. Naiki, K. Higuchi, K. Nakakuki, T. Takeda, *Lab. Invest.* **1991**, *65*, 104–110.
[48] H. LeVine, *Methods Mol. Med. Method. Enzymol.* **1999**, *309*, 274–284.
[49] C. W. Cairo, A. Strzelec, R. M. Murphy, L. L. Kiessling, *Biochemistry* **2002**, *41*, 8620–8629.
[50] Z. Chen, G. Krause, B. Reif, *J. Mol. Biol.* **2005**, *354*, 760–776.
[51] M. Mayer, B. Meyer, *Angew. Chem.* **1999**, *111*, 1902–1906; *Angew. Chem. Int. Ed.* **1999**, *38*, 1784–1788.
[52] Z. Chen, B. Reif, *J. Biomol. NMR* **2004**, *29*, 525–530.
[53] H. LeVine, *Amyloid* **1995**, *2*, 1–6.
[54] A. Lockhart, L. Ye, D. B. Judd, A. T. Merritt, P. N. Lowe, J. L. Morgenstern, G. Hong, A. D. Gee, J. Brown, *J. Biol. Chem.* **2005**, *280*, 7677–7684.
[55] J. B. Robinson, J. M. Strottmann, E. Stellwagen, *Proc. Natl. Acad. Sci. USA* **1981**, *78*, 2287–2291.
[56] O. Mengual, G. Meunier, I. Cayré, K. Puech, P. Snabre, *Colloids Surf. A* **1999**, *152*, 111–123.
[57] O. Mengual, G. Meunier, I. Cayré, K. Puech, P. Snabre, *Talanta* **1999**, *50*, 445–456.
[58] C. Lemarchand, P. Couvreur, M. Besnard, D. Constantini, R. Gref, *Pharm. Res.* **2003**, *20*, 1284–1292.
[59] C. Lemarchand, P. Couvreur, C. Vauthier, D. Constantini, R. Gref, *Int. J. Pharm.* **2003**, *254*, 77–82.
[60] W. B. Russel, D. A. Saville, W. R. Schowalter, *Colloidal Dispersions*, Cambridge University, Cambridge, **1989**.
[61] W. R. Bowen, A. O. Sharif, *Nature* **1998**, *393*, 663–665.
[62] M. A. Moss, M. R. Nichols, D. K. Reed, J. H. Hoh, T. L. Rosenberry, *Mol. Pharmacol.* **2003**, *64*, 1160–1168.
[63] T. L. Lowe, A. Strzelec, L. L. Kiessling, R. M. Murphy, *Biochemistry* **2001**, *40*, 7882–7889.
[64] M. Zarándi, K. Soós, L. Fülöp, Z. Bozsó, Z. Datki, G. K. Tóth, B. Penke, *J. Pept. Sci.* **2007**, *13*, 94–99.
[65] M. Piotto, V. Saudek, V. Sklenar, *J. Biomol. NMR* **1992**, *2*, 661–665.
[66] B. Meyer, T. Peters, *Angew. Chem.* **2003**, *115*, 890–918; *Angew. Chem. Int. Ed.* **2003**, *42*, 864–890.

Received: June 20, 2007
Published online on February 18, 2008

